JOURNAL OF BACTERIOLOGY, Aug. 2009, p. 5123–5133 Vol. 191, No. 16
0021-9193/09/$08.00+0 doi:10.1128/JB.00620-09

Characterization of the *Synechocystis* Strain PCC 6803 Penicillin-Binding Proteins and Cytokinetic Proteins FtsQ and FtsW and Their Network of Interactions with ZipN▽

Martial Marbouty,[1] Khalil Mazouni,[1]† Cyril Saguez,[1] Corinne Cassier-Chauvat,[1,2] and Franck Chauvat[1]*

CEA, iBiTec-S SBIGeM LBI,[1] URA 2096 CNRS,[2] Bat. 142, CEA, Saclay F-91191, Gif sur Yvette CEDEX, France

Received 12 May 2009/Accepted 8 June 2009

Because very little is known about cell division in noncylindrical bacteria and cyanobacteria, we investigated 10 putative cytokinetic proteins in the unicellular spherical cyanobacterium *Synechocystis* strain PCC 6803. Concerning the eight penicillin-binding proteins (PBPs), which define three classes, we found that *Synechocystis* can survive in the absence of one but not two PBPs of either class A or class C, whereas the unique class B PBP (also termed FtsI) is indispensable. Furthermore, we showed that all three classes of PBPs are required for normal cell size. Similarly, the putative FtsQ and FtsW proteins appeared to be required for viability and normal cell size. We also used a suitable bacterial two-hybrid system to characterize the interaction web among the eight PBPs, FtsQ, and FtsW, as well as ZipN, the crucial FtsZ partner that occurs only in cyanobacteria and plant chloroplasts. We showed that FtsI, FtsQ, and ZipN are self-interacting proteins and that both FtsI and FtsQ interact with class A PBPs, as well as with ZipN. Collectively, these findings indicate that ZipN, in interacting with FtsZ and both FtsI and FtQ, plays a similar role to the *Escherichia coli* FtsA protein, which is missing in cyanobacteria and chloroplasts.

The peptidoglycan layer (PG) of bacterial cell wall is a major determinant of cell shape, and the target of our best antibiotics. It is built from long glycan strands of repeating disaccharides cross-linked by short peptides (38). The resultant meshwork structure forms a strong and elastic exoskeleton essential for maintaining shape and withstanding intracellular pressure. Cell morphogenesis and division have been essentially studied in the rod-shaped organisms *Escherichia coli* and *Bacillus subtilis*, which divide through a single medial plane (8, 10, 21, 23). These organisms have two modes of cell wall synthesis: one involved in cell elongation and the second operating in septation (2). Each mode of synthesis is ensured by specific protein complexes involving factors implicated in the last step of PG synthesis (2). The complete assembly of PG requires a glycosyl transferase that polymerizes the glycan strands and a transpeptidase that cross-links them via their peptide side chains (35). Both activities are catalyzed by penicillin-binding proteins (PBPs), which can be divided into three classes: class A and class B high-molecular-weight (HMW) PBPs and class C low-molecular-weight (LMW) PBPs (35).

Class A PBPs exhibit both transglycosylase and transpeptidase activities. In *E. coli*, they seem to be nonspecialized (2), as they operate in the synthesis of both cylindrical wall (cell elongation) and septal PG (cytokinesis). In *B. subtilis*, PBP1 (class A) is partially localized to septal sites and its depletion leads to cell division defects (31).

Class B PBPs, which comprise two proteins in most bacteria, are monofunctional transpeptidases (35), each involved in longitudinal and septal growth of cell wall, respectively (36). In *E. coli*, this protein, PBP3, is also termed FtsI, because it belongs to the *F*ts group of cell division factors whose depletion leads to the *f*ilamentation phenotype (11). These at least 10 Fts proteins are recruited to the division site at mid-cell in the following sequential order: FtsZ, FtsA, ZipA, FtsK, FtsQ, FtsL/FtsB, FtsW, FtsI, and FtsN (11). The cytoplasmic protein FtsZ is the first recruited to the division site, where it polymerizes in a ring-like structure (1), which serves as a scaffold for the recruitment of the other Fts proteins and has been proposed to drive the division process (6). Together the Fts proteins form a complex machine coordinating nucleoid segregation, membrane constriction, septal PG synthesis, and possibly membrane fusion.

Unlike the other PBPs, class C PBPs do not operate in PG synthesis but rather in maturation or recycling of PG during cell septation (35). They are subdivided into four types. Class C type 5 PBP removes the terminal D-alanine residue from pentapeptide side-chains (DD-carboxypeptidase activity). Types 4 and 7 are able to cleave the peptide cross-links (endopeptidase activity). Finally, type AmpH, which does not have a defined enzymatic activity, is believed to play a role in the normal course of PG synthesis, remodeling or recycling (for a review, see reference 35).

In contrast to rod-shaped bacteria, less is known concerning PG synthesis, morphogenesis, and cytokinesis, and their relationships, in spherical-celled bacteria, even though a wealth of them have a strong impact on the environment and/or human health. Furthermore, unlike rod-shaped bacteria spherical-

* Corresponding author. Mailing address: CEA, iBiTec-S SBIGeM LBI, Bat. 142, CEA Saclay F-91191, Gif sur Yvette CEDEX 91191, France. Phone: (33) 1 69 08 78 11. Fax: (33) 1 69 08 47 12. E-mail: franck.chauvat@cea.fr.

† Present address: Laboratoire de Génétique du Développement de la Drosophile, Département de Biologie du Développement, Institut Pasteur 25 rue du Docteur Roux, 75015 Paris, France.

▽ Published ahead of print on 19 June 2009.

celled bacteria possess an infinite number of potential division planes at the point of greater cell diameter, and they divide through alternative perpendicular planes (26, 36, 37, 39). The spherical cells of *Staphylococcus aureus* seem to insert new PG strands only at the septum, and accordingly the unique class A PBP localizes at the septum during cell division (36). In contrast, the rugby-ball-shaped cells of *Streptococcus pneumoniae* synthesize cell wall at both the septum and the neighboring region called "equatorial rings" (36). Accordingly, class A PBP2a and PBP1a were found to operate in elongation and septation, respectively (29).

In cyanobacteria, which are crucial to the biosphere in using solar energy to renew the oxygenic atmosphere and which make up the biomass for the food chain (7, 30, 40), cell division is currently investigated in two unicellular models with different morphologies: the rod-shaped *Synechococcus elongatus* strain PCC 7942 (19, 28) and the spherical-celled *Synechocystis* strain PCC 6803 (26), which both possess a small fully sequenced genome (http://genome.kazusa.or.jp/cyanobase/) that is easily manipulable (18). In both organisms FtsZ and ZipN/Arc6, a protein occurring only in cyanobacteria (ZipN) and plant chloroplasts (Arc6), were found to be crucial for cytokinesis (19, 26, 28) and to physically interact with each other (25, 26). Also, interestingly, recent studies of cell division in the filamentous cyanobacterium *Anabaena* (Nostoc) strain PCC 7120, showed that this process is connected with the differentiation of heterocysts, the cells dedicated to nitrogen fixation (34).

In a continuous effort to study the cell division machine of the unicellular spherical cyanobacterium *Synechocystis*, we have presently characterized its eight presumptive PBPs (22) that define three classes and the putative cytokinetic proteins FtsQ and FtsW, as well as their network of interactions between each other and ZipN. Both FtsI and FtsQ were found to be key players in cell division in interacting with ZipN and class A PBPs. Consequently, ZipN in interacting with FtsZ (26), FtsI, and FtQ, like the FtsA protein of *E. coli*, could play a role similar to FtsA, which is absent in cyanobacteria and chloroplasts.

MATERIALS AND METHODS

Bacterial strains, growth, plasmids, and gene transfer procedures. *Synechocystis* strain PCC 6803 was grown and transformed at 30°C in BG11 medium (33) enriched with 3.78 mM Na_2CO_3, under continuous white light of standard fluence (2,500 lx, 31.25 μE m^{-2} s^{-1}) as described in reference 4. *E. coli* strains TOP10 (Invitrogen), CM404, and DHM1, which were grown on LB (Difco) with or without 1% glucose at 30°C or 37°C, were used for either gene manipulation (TOP10) or the two-hybrid assay (DHM1) (16). The final concentrations of selective antibiotics were as follows: for *E. coli*, ampicillin at 100 μg ml^{-1}, kanamycin at 50 μg ml^{-1}, nalidixic acid at 20 μg ml^{-1}, and spectinomycin at 100 μg ml^{-1} and for *Synechocystis*, kanamycin at 50 to 300 μg ml^{-1}, streptomycin at 5 μg ml^{-1}, and spectinomycin at 2.5 to 10 μg ml^{-1}.

Gene cloning and manipulation. All *Synechocystis* genes surrounded by their flanking regions (about 300 bp), for homologous recombinations mediating targeted gene replacement (20), were amplified by PCR from wild-type (WT) DNA using specific primers. After cloning in the appropriate plasmids (see Table 2), site-directed mutagenesis was performed and disruptions were made through standard PCR-driven overlap extension (13). We used deletion cassettes that carry the antibiotic-resistant marker inserted in the same orientation as the gene to be inactivated and verified their DNA sequences (Big Dye kit; ABI Perkin Elmer).

Microscopy. A total of 1.25×10^5 *Synechocystis* cells from mid-log-phase culture were placed on microscope slides and immobilized by a 5- to 10-min incubation at room temperature. Images were captured with a Leica DMRXA microscope equipped with a ×100 oil immersion lens, a Ropper Scientific Micromax cooled charge-coupled device camera, and Metamorph software (Universal Imaging). The final processing of images for presentation was done using Adobe Photoshop.

FACS analysis. Cells from mid-log-phase liquid cultures were harvested, washed twice, and resuspended in phosphate-buffered saline (Sigma-Aldrich) to a final optical density at 580 nm of 0.3 (1.5×10^7cells ml^{-1}). Then, 2×10^4 cells were analyzed by using a FACSCalibur fluorescence-activated cell sorting (FACS) cytometer (Becton Dickinson) with the following settings: forward scatter (FCS), E01 log; side scatter, 350 V. Results were collected with CellQuest software, version 3.1 (Becton Dickinson). Data were plotted on a two-dimensional graph (*x* axis, FSC; *y* axis, number of cells). Then histograms from WT and mutant strains were superimposed. Experiments were repeated twice.

The *E. coli* BACTH assay. The bacterial two-hybrid (BACTH) system (16) is composed of two replication-compatible plasmids, pKT25 and pUT18, encoding the intrinsically inactive N-terminal T25 domain and C-terminal T18 domain of the adenylate cyclase (AC) from *Bordetella pertussis*, as well as an *E. coli* reporter strain, DHM1, deficient in the endogenous cyclic AMP-producing enzyme. When the coding sequences for physically interacting proteins are cloned in pKT25 and pUT18 and subsequently coexpressed in DHM1, their interaction restores AC activity. This turns on the production of the β-galactosidase (β-Gal) reporter enzyme, leading to the blue-colored colonies on LB indicator plates containing 40 μg ml^{-1} X-Gal (5-bromo-4-chloro-3-indolyl-β-D-galactopyranoside; Eurobio), 0.5 mM IPTG (isopropyl-β-D-thiogalactopyranoside; Invitrogen), ampicillin, kanamycin, and nalidixic acid. To reduce the number of cloning experiments, we constructed a slightly modified variant of pUT18 we termed pUT18m1, in which the T18 domain is followed by the same multiple cloning site as the one that follows the T25 domain of AC in pKT25. All *Synechocystis* open reading frames, were cloned as PstI-BamHI restriction fragments (or NsiI and BglII when they possessed internal PstI or BamHI sites) in the PstI-BamHI sites of the reporter plasmids pKT25 and pUT18m1. DHM1 cells doubly transformed with pKT25- and pUT18m1-derived plasmids (Table 2) were incubated for 2 days at 30°C on LB supplemented with glucose 1% (to allow repression of the *lac* promoter), ampicillin, and kanamycin. Production of the β-Gal reporter enzyme was monitored as follows. Cells grown overnight (16 h) at 30°C in LB–0.5 mM IPTG were harvested by centrifugation (10 min at 5,000 rpm), washed with lysis buffer (50 mM Tris HCl [pH 8.0], 50 mM NaCl), resuspended in ice-cold lysis buffer containing 2 mM phenylmethylsulfonyl, and homogenized for 5 min on ice. They were then incubated with 1 mg ml^{-1} lysozyme for 1 h on ice and disrupted by sonication (three 10-s pulses at power 6 on a Microson apparatus; Misonix). The lysates were cleared by centrifugation at 12,000 × *g* for 30 min at 4°C, and proteins of the soluble extracts were quantified by Bradford assay (Bio-Rad). Then, aliquots (1 to 10 μl) of soluble proteins were added to 0.8 ml of Z buffer (60 mM Na_2HPO_4, 40 mM NaH_2PO4 [pH 7.5], 1 mM $MgSO_4$, 50 mM β-mercaptoethanol), and the β-Gal reaction was started by adding 0.2 ml of *o*-nitrophenol-β-galactoside (ONPG) at 4 mg ml^{-1} in Z buffer lacking β-mercaptoethanol. The reaction was stopped after 3 min with 0.5 ml of 1 M Na_2CO_3 and A_{420} was recorded. One β-Gal unit = 1 nmol of ONPG min^{-1} mg^{-1} protein.

RESULTS

Construction of *Synechocystis* mutants lacking or depleted in PBPs. As very little is known concerning PBPs in noncylindrical bacteria and cyanobacteria, we investigated the role of the eight proteins of the spherical-celled cyanobacterium *Synechocystis* strain PCC 6803 that share sequence homology with *E. coli* PBPs (22). These *Synechocystis* proteins are namely the class A-related PBP1, PBP2, and PBP3; the unique class B member, PBP4 (also termed FtsI); the class C type 4 homologs PBP5 and PBP8; and the class C PBPs type AmpH members PBP6 and PBP7 (Table 1). We constructed *pbp* gene deletion cassettes (Table 2) (see Materials and Methods), in which each protein coding sequence has been replaced by a transcription terminatorless marker gene for selection, while preserving the flanking DNA regions for homologous recombinations mediating targeted gene replacement in *Synechocystis* (20). After transformation in *Synechocystis*, which harbors about 10 chromosome copies per cell (20), we verified through PCR and DNA sequencing that the marker gene had been properly

TABLE 1. Presumptive PBPs in *Synechocystis*

Type	Name[a]	Gene identification no.[b]
HMW		
Class A	PBP1	sll0002
Class A	PBP2	slr1710
Class A	PBP3	sll1434
Class B	PBP4/FtsI	sll1833
LMW		
Class C type 4	PBP5	slr0646
Class C type 4	PBP8	slr0804
Class C type AmpH	PBP6	sll1167
Class C type AmpH	PBP7	slr1924

[a] Proposed in reference 22.
[b] Gene identifier in CyanoBase.

inserted in the *Synechocystis* chromosome, in place of the studied gene, and we assayed whether the segregation between WT and mutant chromosome copies was complete (the studied gene is dispensable to cell growth) or not (the studied gene is essential to cell viability). All three Δ*pbp1*::Km^r, Δ*pb2*::Km^r, and Δ*pbp3*::Km^r mutants retained no WT chromosome copies (data not shown) and grew as fit as the WT strain (Table 3 and Fig. 1) showing that each of the three class A PBPs is dispensable for *Synechocystis* viability.

***Synechocystis* can survive in the absence of one but not two class A PBPs.** To test whether the three genes possess overlapping functions, we attempted to construct all three double mutants lacking any pair combination of the three class A PBPs. Interestingly, all double mutants invariably died upon restreaking onto selective medium containing both selective antibiotics kanamycin and streptomycin (or spectinomycin), showing that *Synechocystis* requires at least two HMW PBP class A proteins to survive. Taken together, our results indicate that class A PBPs exhibit crucial and partially overlapping functions.

The absence of PBP2, but not of the other two class A PBPs, PBP1 and PBP3, leads to minicells. To investigate the impact of each class A PBP on *Synechocystis* cell morphogenesis, we observed the three Δ*pbp1*::Km^r, Δ*pbp2*::Km^r, and Δ*pbp3*::Km^r single mutants through phase-contrast microscopy. Both Δ*pbp1*::Km^r and Δ*pbp3*::Km^r cells retained normal morphology, whereas Δ*pbp2*::Km^r cells were found to be significantly smaller than WT cells (Fig. 2A). We then confirmed these results using FACS flow cytometry (Fig. 2B), a quantitative evaluation of cell shape (27) that measures the FSC value that is proportional to cell size. In agreement with our microscopy observation, the mean FSC value of Δ*pbp2*::Km^r cells (48.92) appeared to be significantly smaller than those of WT, Δ*pbp1*::Km^r, and Δ*pbp3*::Km^r cells (mean FSC values of 75.94, 74.59, and 73.84, respectively). These findings suggest that PBP2 operates in the synthesis of PG required for normal cell growth of *Synechocystis*.

FtsI, the unique class B PBP, is indispensable to *Synechocystis*: its depletion leads to giant cells. We then studied the role of FtsI, the unique class B PBP (Table 1), using the techniques described above, and found FtsI to be essential to *Synechocystis* viability. The resulting FtsI-depleted Δ*ftsI*::Km^r/*ftsI*$^+$ mutant grew more slowly (doubling time of about 15 h) (Table 3) than the WT strain (doubling time of about 10 h). This finding cannot be interpreted in term of a reduced initiation of cytokinesis in the FtsI-depleted mutant, as the fraction of its dividing cells remained similar to, if not higher than, that in the WT strain (71% and 60%, respectively) (Fig. 1). Instead, it is the completion of cytokinesis (i.e., the septation) which seemed to be slower in the FtsI-depleted cells. Indeed, FtsI-depleted cells displayed an increased size (Fig. 2A) and, accordingly, a higher FSC value (152.15) (Fig. 2B) than WT cells (75.94). Furthermore, FtsI depletion led to cloverleaf-like clusters of four large unseparated cells (Fig. 1 and 2) not observed in WT cells. These cloverleaf-like cell clusters likely result from the delayed septation of daughter cells, which was not completed before the initiation of the second round of division. Collectively, our results suggest that FtsI plays a crucial role in the inward synthesis of PG required for completing septation.

***Synechocystis* can survive in the absence of one but not the two class C type 4 PBPs, PBP5 and PBP8, operating in septation.** We then studied the role of PBP5 and PBP8, the two class C type 4 PBPs (Table 1). Both appeared to be dispensable to *Synechocystis* growth (Table 3) and morphology (Fig. 1 and Fig. 3), likely because they have redundant functions. Indeed, it was not possible to obtain the double-deletion mutant lacking both PBP5 and PBP8, irrespective of the sequential order of attempted double deletions, i.e., tentative deletion of either *pbp8* in Δ*pbp5* null recipient cells or *pbp5* in Δ*pbp8* null cells. All resulting cells remained heteroploids in retaining the ability to encode either PBP5 or PBP8 and behaved similarly. They all grew about twice as slowly as WT cells (Table 3), likely because their septation was slow, as suggested by the occurrence of a high proportion (25%) (Fig. 1) of cloverleaf-like four-cell clusters (Fig. 3A) accounting for the observed high FCS value (mean, 148.94) (Fig. 3B), compared to that in WT cells (mean, 75.94). These findings suggest that PBP5 and PBP8, the two class C type 4 PBPs, are required for completion of the septation enabling daughter cell separation.

***Synechocystis* can survive in the absence of one but not both class C type AmpH PBPs, PBP6 and PBP7, the combined depletion of which generates giant cells.** The two *Synechocystis* class C type AmpH PBPs (Table 1) PBP6 and PBP7 appeared to be dispensable to cell growth (Table 3) and morphology (Fig. 1 and 4), likely because they share redundant functions. Indeed, it was not possible to construct the double-deletion mutant lacking both PBP6 and PBP7, irrespective of the sequential order of the attempted double deletion: i.e., tentative deletion of either *pbp7* in Δ*pbp6* null cells or *pbp6* in Δ*pbp7* null cells. Both resulting heteroploid strains retained the ability to encode either PBP6 or PBP7 and behaved similarly. They grew about twice as slowly as WT cells (Table 3) and generated giant cells (Fig. 4A), likely accounting for the high FCS value (mean, 186.42) of these mutants (Fig. 4B), compared to WT cells (mean, 75.94). We did not observe cloverleaf-like four-cell clusters, unlike the abovementioned cells depleted for the two class C type 4 PBPs.

Both FtsQ and FtsW are indispensable to *Synechocystis*: their depletion leads to giant cells. As we found FtsI to be indispensable to *Synechocystis*, we decided to investigate the role of both FtsQ (Sll1632) and FtsW (Slr1267) homolog proteins, because both FtsQ and FtsW were shown in *E. coli* to

TABLE 2. Characteristics of the plasmids used in this study

Plasmid	Relevant feature(s)[a]	Source or reference
pGEMT	AT overhang Amp^r cloning vector	Promega
pUC4K	Source of the Km^r marker gene	Pharmacia
pHPΩ45	Source of the Sm^r Sp^r marker gene	32
ppbp1	pGEMT with the *Synechocystis pbp1* gene and its flanking sequences, where part of the PBP1 CS (from bp 84 to 2424) was replaced by a SmaI site	This study
pΔ*pbp1*::Km^r	ppbp1 with the Km^r marker inserted in the unique SmaI site	This study
pΔ*pbp1*::Sm^{r}Sp^r	ppbp1 with the Sm^r Sp^r marker inserted in the unique SmaI site	This study
ppbp2	pGEMT with the *Synechocystis pbp2* gene and its flanking sequences, where part of the PBP2 CS (from bp 111 to 2037) was replaced by a SmaI site	This study
pΔ*pbp2*::Km^r	ppbp2 with the Km^r marker inserted in the unique SmaI site	This study
pΔ*pbp2*::Sm^{r}Sp^r	ppbp2 with the Sm^r Sp^r marker inserted in the unique SmaI site	This study
ppbp3	pGEMT with the *Synechocystis pbp3* gene and its flanking sequences, where part of the PBP3 CS (from bp 180 to 1734) was replaced by a SmaI site	This study
pΔ*pbp3*::Km^r	ppbp3 with the Km^r marker inserted in the unique SmaI site	This study
pΔ*pbp3*::Sm^{r}Sp^r	ppbp3 with the Sm^r Sp^r marker inserted in the unique SmaI site	This study
pftsI	pGEMT with the *Synechocystis ftsI* gene and its flanking sequences, where part of the FtsI CS (from bp 129 to 1701) was replaced by a SmaI site	This study
pΔ*ftsI*::Km^r	pftsI with the Km^r marker inserted in the unique SmaI site	This study
ppbp5	pGEMT with the *Synechocystis pbp5* gene and its flanking sequences, where part of the PBP5 CS (from bp 129 to 1326) was replaced by a SmaI site	This study
pΔ*pbp5*::Km^r	ppbp5 with the Km^r marker inserted in the unique SmaI site	This study
ppbp6	pGEMT with the *Synechocystis pbp6* gene and its flanking sequences, where part of the PBP6 CS (from bp 78 to 1,098) was replaced by a SmaI site	This study
pΔ*pbp6*::Km^r	ppbp6 with the Km^r marker inserted in the unique SmaI site	This study
ppbp7	pGEMT with the *Synechocystis pbp7* gene and its flanking sequences, where part of the PBP7 CS (from bp 129 to 1602) was replaced by a SmaI site	This study
pΔ*pbp7*::Kmr	ppbp7 with the Km^r marker inserted in the unique SmaI site	This study
pΔ*pbp7*::Sm^{r}Sp^r	ppbp7 with the Sm^r Sp^r marker inserted in the unique SmaI site	This study
ppbp8	pGEMT with the *Synechocystis pbp8* gene and its flanking sequences, where part of the PBP8 CS (from bp 72 to 876) was replaced by a SmaI site	This study
pΔ*pbp8*::Km^r	ppbp8 with the Km^r marker inserted in the unique SmaI site	This study
pΔ*pbp8*::Sm^{r}Sp^r	ppbp8 with the Sm^r Sp^r marker inserted in the unique SmaI site	This study
pftsQ	pGEMT with the *Synechocystis ftsQ* gene and its flanking sequences, where part of the FtsQ CS (from bp 138 to 663) was replaced by a SmaI site	This study
pΔ*ftsQ*::Km^r	pftsQ with the Km^r marker inserted in the unique SmaI site	This study
pftsW	pGEMT with the *Synechocystis ftsW* gene and its flanking sequences, where part of the FtsW CS (from bp 96 to 1029) was replaced by a SmaI site	This study
pΔ*ftsW*::Km^r	pftsW with the Km^r marker inserted in the unique SmaI site	This study
pKT25	Km^r plasmid encoding the N-terminal T25 domain (amino acids 1-224) of the *B. pertussis* AC in frame with a downstream multiple cloning site	16
pKT25-*zip*	pKT25 with the leucine zipper domain of the yeast GCN4 activator	16
pKT25-*zipN*	pKT25 with the full-length *Synechocystis zipN* CS	This study
pKT25-*ftsQ*	pKT25 with the full-length *Synechocystis ftsQ* CS	This study
pKT25-*ftsW*	pKT25 with the full-length *Synechocystis ftsW* CS	This study
pKT25-*ftsI*	pKT25 with the full-length *Synechocystis ftsI* CS	This study
pKT25-*pbp1*	pKT25 with the full-length *Synechocystis pbp1* CS	This study
pKT25-*pbp2*	pKT25 with the full-length *Synechocystis pbp2* CS	This study
pKT25-*pbp3*	pKT25 with the full-length *Synechocystis pbp3* CS	This study
pKT25-*pbp5*	pKT25 with the full-length *Synechocystis pbp5* CS	This study
pKT25-*pbp6*	pKT25 with the full-length *Synechocystis pbp6* CS	This study
pKT25-*pbp7*	pKT25 with the full-length *Synechocystis pbp7* CS	This study
pKT25-*pbp8*	pKT25 with the full-length *Synechocystis pbp8* CS	This study
pUT18	Amp^r plasmid encoding the T18 domain (amino acids 225-339) of the *B. pertussis* AC in frame with an upstream multiple cloning site	16
pUT18-*zip*	pUT18 with the leucine zipper domain of the yeast GCN4 activator	16
pUT18m1	pUT18 derivative encoding the AC T18 domain in frame with a downstream multiple cloning site identical to that of pKT25	This study
pUT18m1-*zipN*	pUT18m1 with the full-length *Synechocystis zipN* CS	This study
pUT18m1-*ftsQ*	pUT18m1 with the full-length *Synechocystis ftsQ* CS	This study
pUT18m1-*ftsW*	pUT18m1 with the full-length *Synechocystis ftsW* CS	This study
pUT18m1-*ftsI*	pUT18m1 with the full-length *Synechocystis ftsI* CS	This study
pUT18m1-*pbp1*	pUT18m1 with the full-length *Synechocystis pbp1* CS	This study
pUT18m1-*pbp2*	pUT18m1 with the full-length *Synechocystis pbp2* CS	This study
pUT18m1-*pbp3*	pUT18m1 with the full-length *Synechocystis pbp3* CS	This study
pUT18m1-*pbp5*	pUT18m1 with the full-length *Synechocystis pbp5* CS	This study
pUT18m1-*pbp6*	pUT18m1 with the full-length *Synechocystis pbp6* CS	This study
pUT18m1-*pbp7*	pUT18m1 with the full-length *Synechocystis pbp7* CS	This study
pUT18m1-*pbp8*	pUT18m1 with the full-length *Synechocystis pbp8* CS	This study

[a] CS, protein coding sequence; Δ, deletion.

TABLE 3. Characteristics of the mutants constructed in this study

Gene inactivated	Dispensability	Doubling time of growing cells (h)
None		10 ± 1
ftsQ	No	16 ± 1
ftsW	No	15 ± 1
pbp1	Yes	10 ± 1
pbp2	Yes	10 ± 1
pbp3	Yes	10 ± 1
pbp4 (*ftsI*)	No	15 ± 1
pbp5	Yes	10 ± 1
pbp6	Yes	10 ± 1
pbp7	Yes	10 ± 1
pbp8	Yes	10 ± 1
pbp5 and *pbp8*	No	21 ± 2
pbp6 and *pbp7*	No	19 ± 2

interact with FtsI (3) and to be involved in FtsI recruitment to the division site (11). We found that both *ftsQ* and *ftsW* are essential to cell viability in *Synechocystis* (Table 3). The resulting Δ*ftsQ*::Km^r/*ftsQ*$^+$ and Δ*ftsW*::Km^r/*ftsW*$^+$ heteroploid mutants grew more slowly than the WT strain (respective doubling times of 16 h, 15 h, and 10 h) (Table 3) and generated giant cells (Fig. 5) (FCS values of 153.74 and 154.46 for Δ*ftsQ*::Km^r/*ftsQ*$^+$ and Δ*ftsW*::Km^r/*ftsW*$^+$ cells, respectively), like the Δ*ftsI*::Km^r/*ftsI*$^+$ mutant (doubling time of about 15 h and FCS value of about 152.15).

Characterization of the interaction network among PBPs, FtsQ, FtsW, and ZipN. To characterize the interplay between PG synthesis (PBPs) and cytokinesis (Fts proteins), we investigated the pairwise interactions between the presently studied PBPs, FtsQ, FtsW, and ZipN, the previously described cytokinetic factor (26). For this purpose, we used the BACTH system (16), which worked well with cell division proteins from both *Synechocystis* (26) and *E. coli* (5, 15), including membrane-associated proteins (17). Full-length coding sequences for the studied *Synechocystis* proteins were cloned in the two BACTH reporter plasmids pKT25 and pUT18m1 (see Materials and Methods) (Table 2), which were subsequently cotransformed to *E. coli* to search for pairwise interactions restoring the production of the β-Gal enzyme (Fig. 6). All pairwise interactions were observed in both mutually confirmatory combinations, thereby strengthening their biological relevance. The only exception was FtsW, for which only the T25-FtsW fusion protein, not the T18-FtsW hybrid, led to detection of FtsW partner, as previously reported for the *E. coli* FtsW protein (15). We found that FtsI, FtsQ, and ZipN are self-interacting proteins (Fig. 6), as observed for *E. coli* proteins FtsQ (15) and FtsI (24), and Arc6, the chloroplast ortholog of ZipN (25). Also interestingly, FtsI and FtsQ were found to interact with each other (Fig. 6), like their *E. coli* counterparts (3, 15), as well as with PBP1 and PBP3, which both appeared to interact with PBP2. Furthermore, both FtsI and FtsQ were found to interact with ZipN, the FtsZ-interacting protein occurring only in cyanobacteria (26) and plant chloroplasts (9). Collectively, these findings demonstrate that both FtsI and FtsQ are key players in cyanobacterial cell division. In addition, they suggest (Fig. 7) that ZipN could play a similar role to the *E. coli* FtsA protein (which is absent from cyanobacteria and chloroplasts),

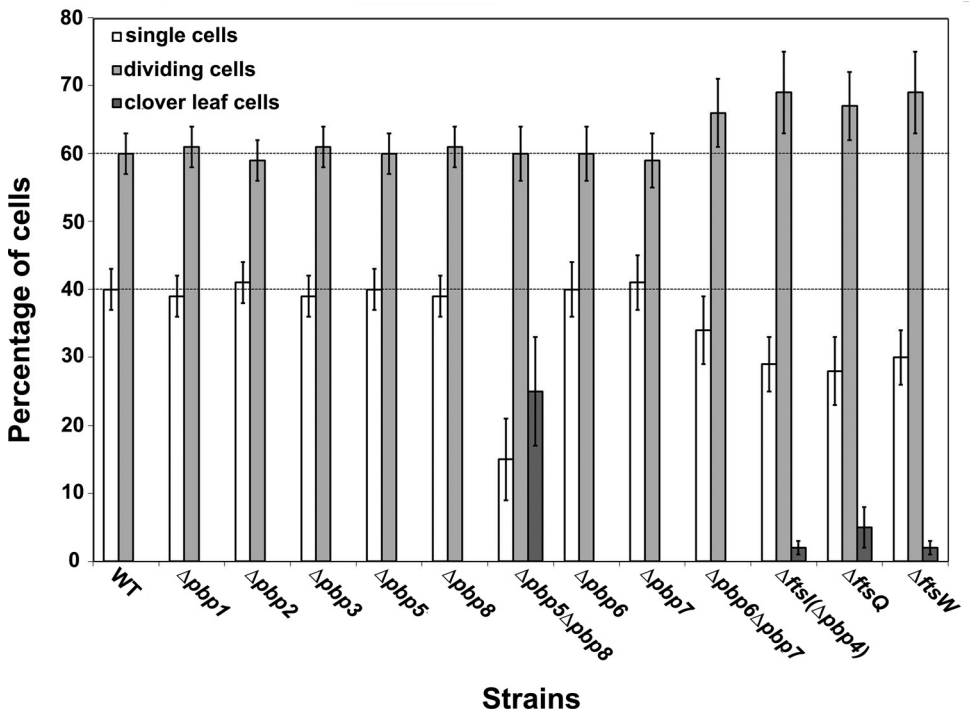

FIG. 1. Proportions of various cell types observed in the *Synechocystis* mutants constructed in this study. In each case, at least 200 randomly chosen cells were classified in the following three categories: single cells, doublets of dividing cells, and cloverleaf-type cell aggregates. Strains are indicated on the *x* axis, and the percentage of each category is indicated on the *y* axis (error bars represent the standard deviation). These experiments were performed twice with two independent clones harboring the same mutation.

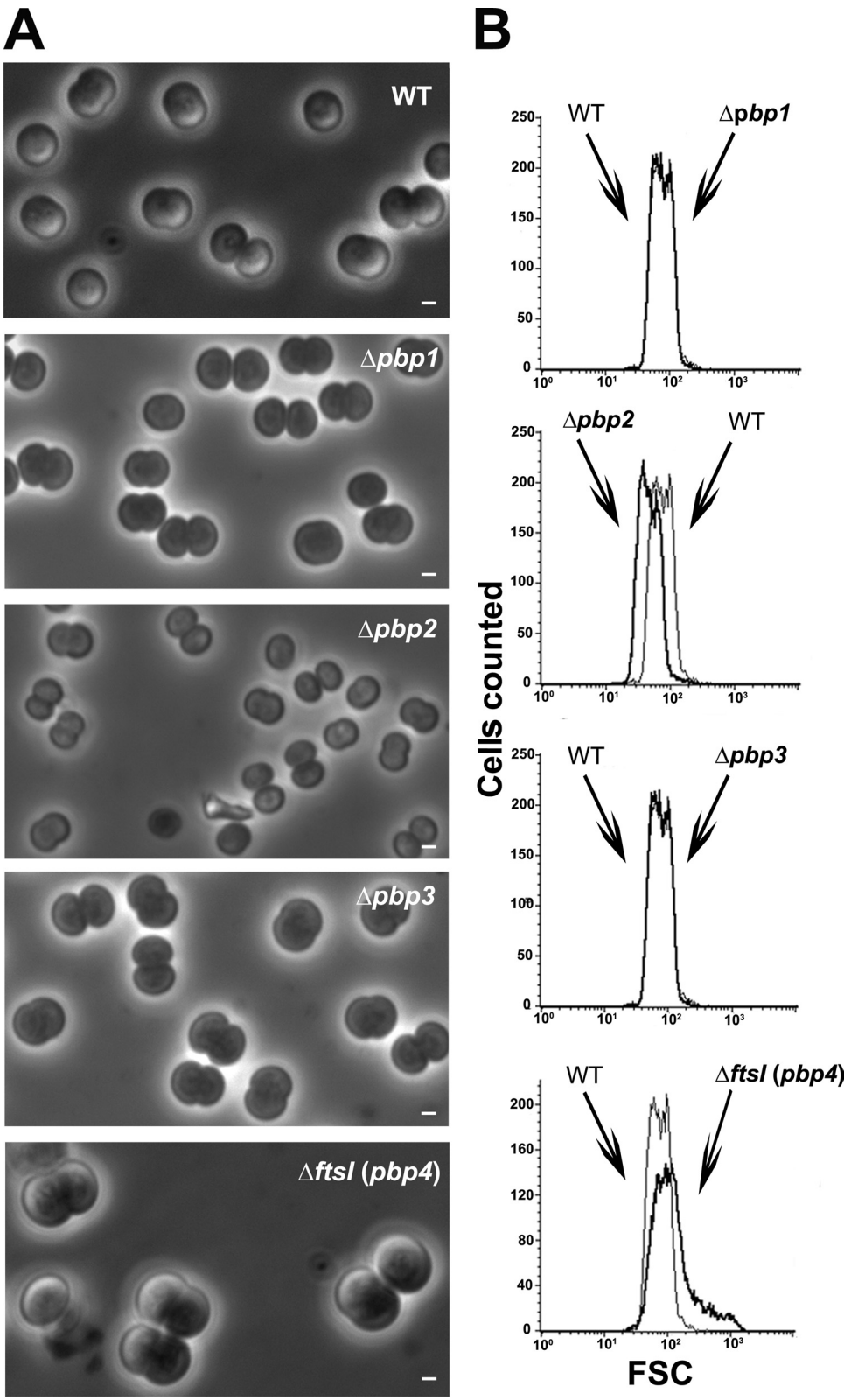

FIG. 2. Morphology of *Synechocystis* mutant cells depleted in the PBPs of either class A or B. Shown are a phase-contrast image (A; scale bar = 1 μm) and flow cytometry analysis (B) of WT or mutant (Δ) cells totally or partially lacking (Table 3) the indicated PBP. For each mutant, the FSC histogram (bold lines) has been overlaid with that of the WT to better visualize the influence of the mutation on cell size. These experiments were performed twice with two independent clones harboring the same mutation.

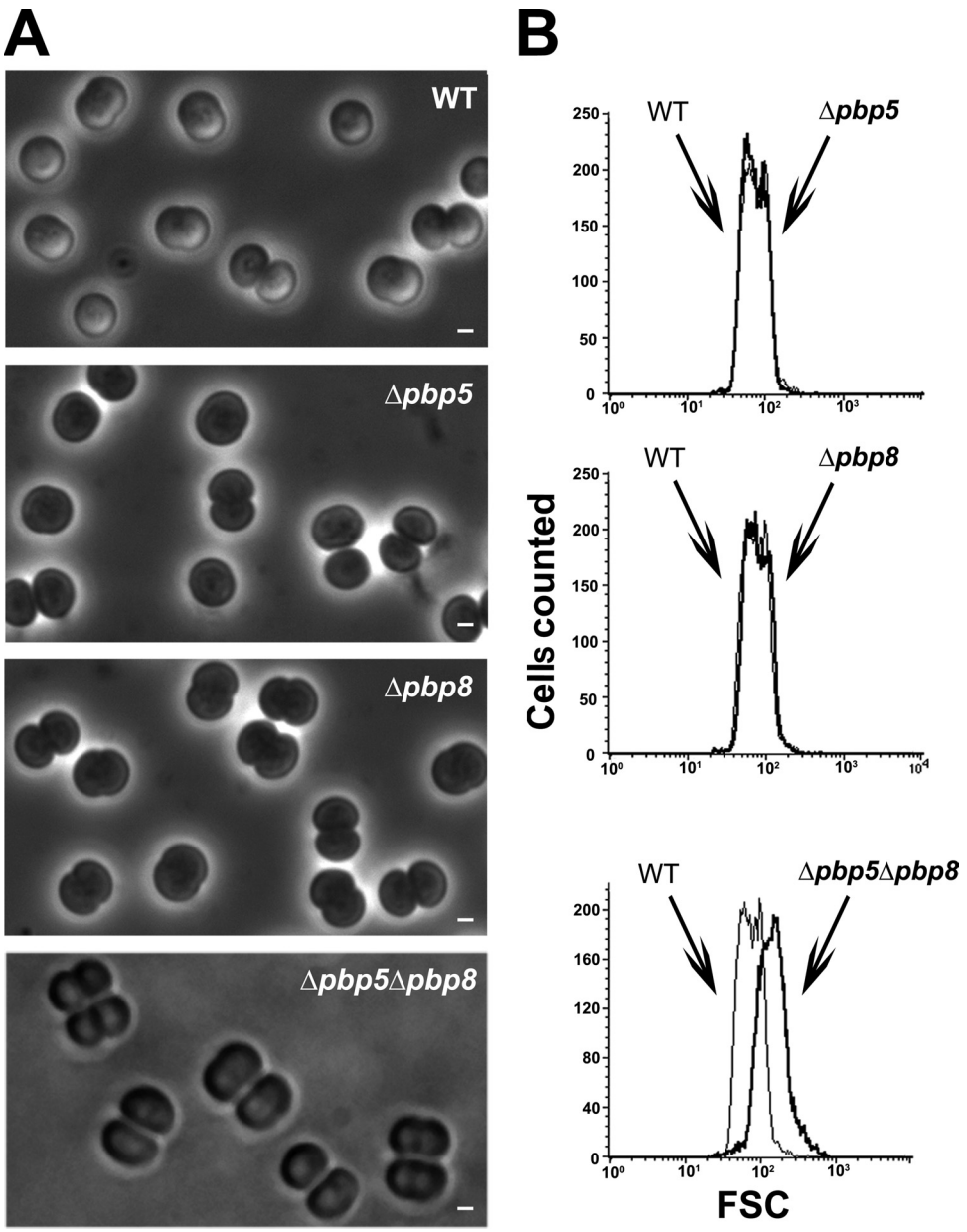

FIG. 3. Morphology and size of *Synechocystis* mutant cells depleted in class C type 4 PBPs. Shown are a phase-contrast image (A; scale bar = 1 μm) and flow cytometry analysis (B) of WT or mutant (Δ) cells totally or partially lacking (Table 3) the indicated PBP. For each mutant, the FSC histogram (bold lines) has been overlaid with that of the WT to better visualize the influence of the mutation on cell size. These experiments were performed twice with two independent clones harboring the same mutation.

which interacts with FtsZ (11) and both FtsI and FtQ (3, 15). We also found that *Synechocystis* FtsW interacts with FtsI, as reported in *E. coli* (15). We observed no interaction with class C PBPs, possibly because these proteins might localize to the periplasm (35), thereby negatively influencing the accumulation and/or activity of the recreated AC reporter enzyme.

DISCUSSION

As very little is known concerning cell division in noncylindrical bacteria and cyanobacteria, we have investigated several putative cytokinetic proteins in the unicellular spherical cyanobacterium *Synechocystis* strain PCC 6803. We focused on the eight presumptive PBP-like proteins (22): the three class A PBPs, PBP1, PBP2 and PBP3; the unique class B PBP, FtsI (PBP4); the two class C type 4 PBPs, PBP5 and PBP8; and the two class C type AmpH PBPs, PBP6 and PBP7 (Table 1). We found that *Synechocystis* can survive without one but not two class A PBPs (Table 3) and that PBP2 is likely involved in the synthesis of PG required for normal cell growth since it leads to minicells. In contrast, both PBP1 and PBP3 appeared to be less important than PBP2 as their absence has no obvious phenotype (Fig. 2).

The unique class B PBP protein, FtsI (PBP4), appeared to

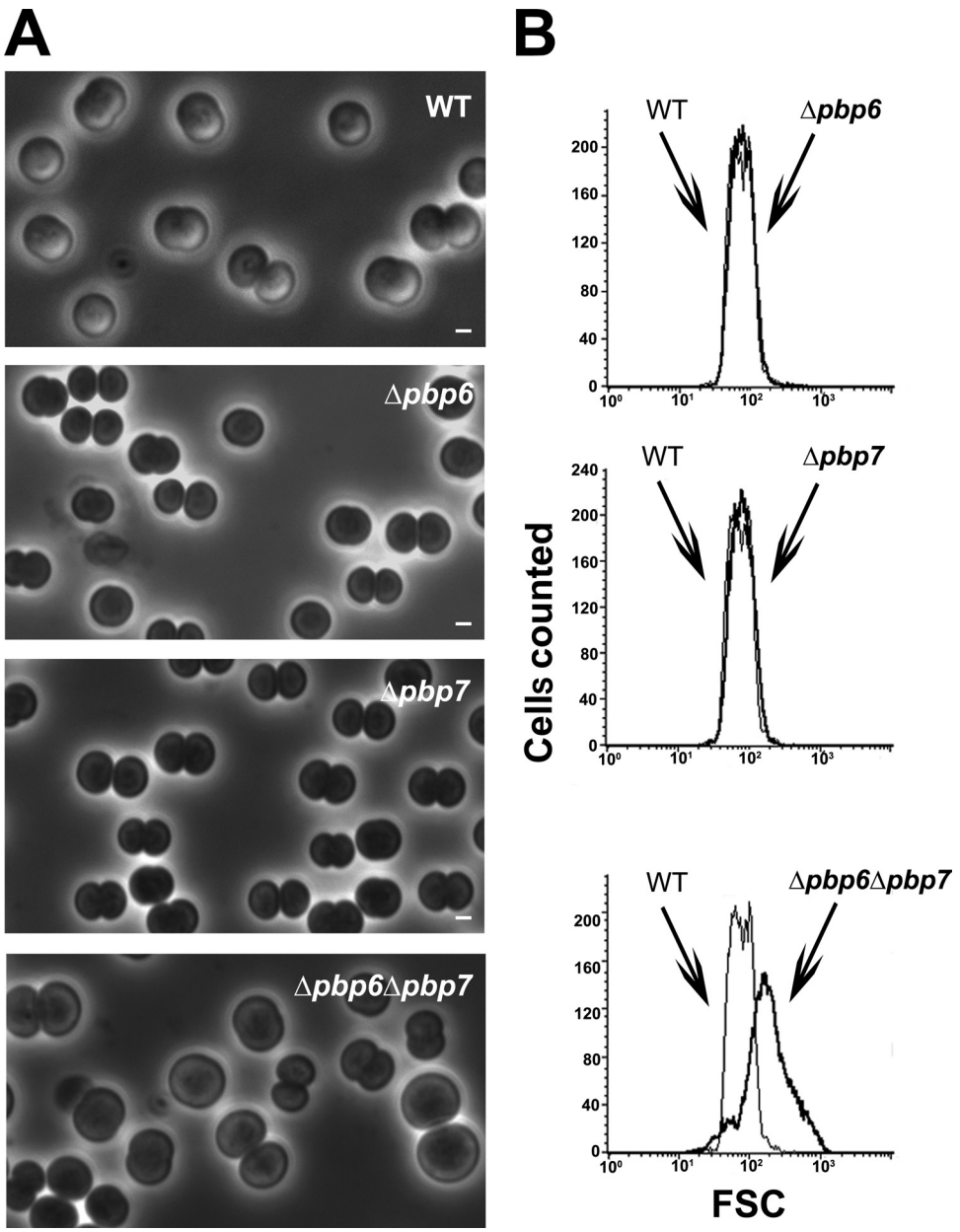

FIG. 4. Morphology and size of *Synechocystis* mutant cells depleted in class C type AmpH PBPs. Shown are a phase-contrast image (A; scale bar = 1 μm) and flow cytometry analysis (B) of WT or mutant (Δ) cells totally or partially lacking (Table 3) the indicated PBP. For each mutant, the FSC histogram (bold lines) has been overlaid with that of the WT to better visualize the influence of the mutation on cell size. These experiments were performed twice with two independent clones harboring the same mutation.

be indispensable to *Synechocystis*. The resulting heteroploid strain (Δ*ftsI*::Km^r/*ftsI*$^+$) displayed giant cells and cloverleaf-like clusters of four large unseparated cells (Fig. 1 and 2). These cloverleaf-like cell clusters likely result from the delayed septation of daughter cells, which was not completed before the initiation of the second round of division. Collectively, our findings suggest that FtsI might operate in the inward synthesis or incorporation of PG at the septum required for completing separation of daughter cells.

As observed for class A PBPs, we found that *Synechocystis* can survive without one but not the two class C PBPs of either type 4 (PBP5 and PBP8) or type AmpH (PBP6 and PBP7). Interestingly, the heteroploid mutants resulting from the attempted double deletion of the genes encoding PBP5 and PBP8 on one hand or PBP6 and PBP7 on the other hand grew slowly (Table 3) and displayed giant cells (Fig. 3 and 4), like the Δ*ftsI*::Km^r/*ftsI*$^+$ heteroploid strain (Table 3 and Fig. 2). Interestingly, the mutants depleted of both PBP5 and PBP8, but not of both PBP6 and PBP7, exhibit a high proportion of cloverleaf-like four-cell clusters (Fig. 1, 3, and 4). These findings suggest that PBP5 and PBP8, but not PBP6 and PBP7, are involved in the completion of the septation allowing daughter cell separation, like FtsI.

We think that the giant morphology of spherical cells results

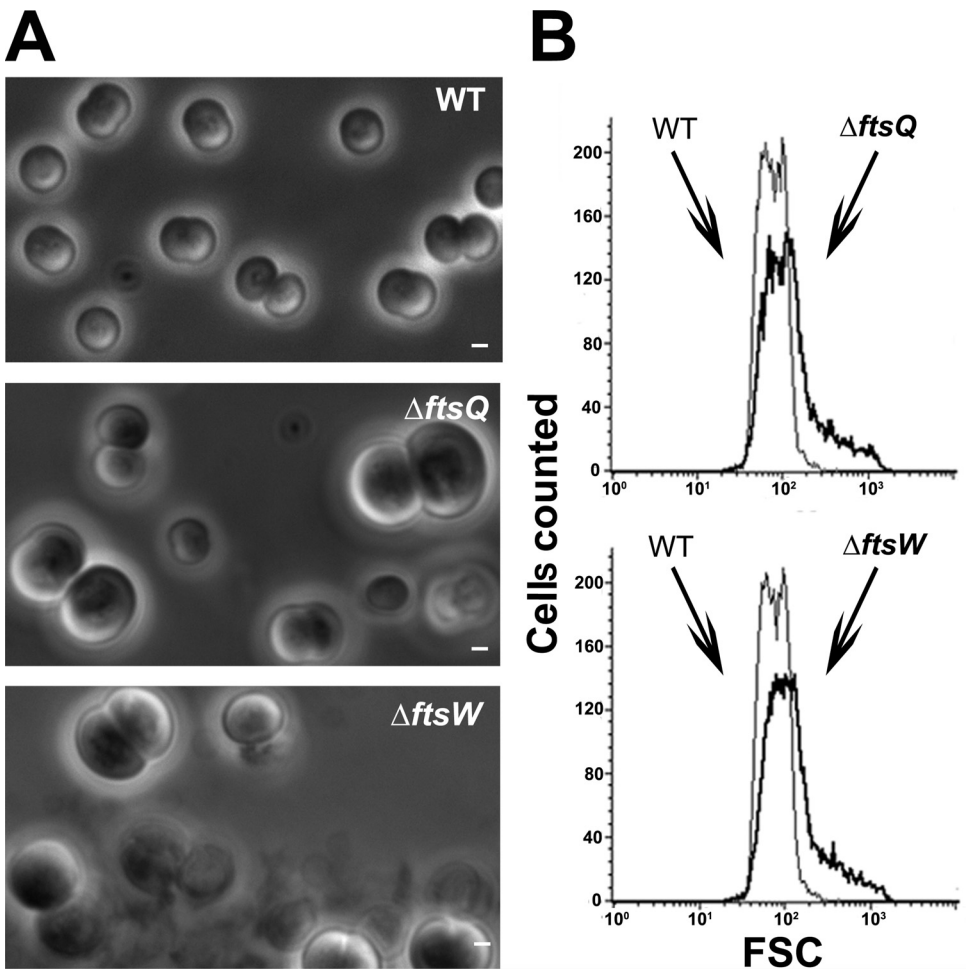

FIG. 5. Morphology and size of *Synechocystis* mutant cells depleted in proteins FtsQ and FtsW. Shown are a phase-contrast image (A; scale bar = 1 μm) and flow cytometry analysis (B) of WT or mutant (Δ) cells lacking the indicated protein. For each mutant, the FSC histogram (bold lines) has been overlaid with that of the WT to better visualize the influence of the mutation on cell size. These experiments were performed twice with two independent clones harboring the same mutation.

from their septation being slowed down more importantly than their growth. This interpretation is supported by the finding that the specific inhibition of Z-ring assembly by the antibacterial compound PC190723 causes dramatic enlargement of the spherical-celled organism *S. aureus* (12). In contrast, in a rod-shaped bacterium such as *E. coli*, when septation is more affected than cell growth (14), the corresponding *fts* mutants become filamentous (8, 10, 21, 23). To confirm that the giant-cell phenotype in a spherical-celled organism is equivalent to the filamentous phenotype of a rod-shaped organism, we studied the impact on *Synechocystis* of the depletion of the FtsQ and FtsW homologs, because their depletion in *E. coli* triggers filamentation. The other reason why we studied the presumptive *Synechocystis* FtsQ and FtsW proteins is that in *E. coli* both FtsQ and FtsW were found to interact with FtsI (3). First, we found that both the cyanobacterial FtsQ and FtsW are indispensable to *Synechocystis*, like FtsI. Then, as expected, we found that both the FtsQ- and FtsW-depleted mutants exhibit similar defects to FtsI: i.e., they grow slowly (Table 3) and display giant cells (Fig. 3 and 5). Furthermore, we used a convenient BACTH system to show that both FtsQ and FtsW physically interact with FtsI, as observed in *E. coli*. We also used this two-hybrid system to characterize the interplay between PG synthesis (PBPs) and cytokinesis (Fts proteins). We also included the ZipN protein in our study because it is the crucial FtsZ partner in cyanobacteria (26) and plant chloroplasts, where it is termed "Arc6" (9). Interestingly, we found that FtsI, FtsQ, and ZipN are self-interacting proteins (Fig. 6), as observed for *E. coli* proteins FtsI and FtsQ (24) and chloroplastic protein Arc6 (25). Also interestingly, we found that both FtsI and FtsQ interact with ZipN, as well as with PBP1 and PBP3, which both appeared to interact with PBP2 (Fig. 6). Consequently, both FtsI and FtsQ appeared to be key players in cyanobacterial cell division. Collectively, our findings (Fig. 7) indicate that ZipN, in interacting with FtsZ (26) and both FtsI and FtQ (this study), plays a role similar to the *E. coli* FtsA protein, which is absent from cyanobacteria and chloroplasts. The *E. coli* FtsA protein assembles at the Z ring early and participates in the sequential recruitment of the Fts proteins, including both FtsI and FtsQ (6), which interact directly with FtsA (3, 15).

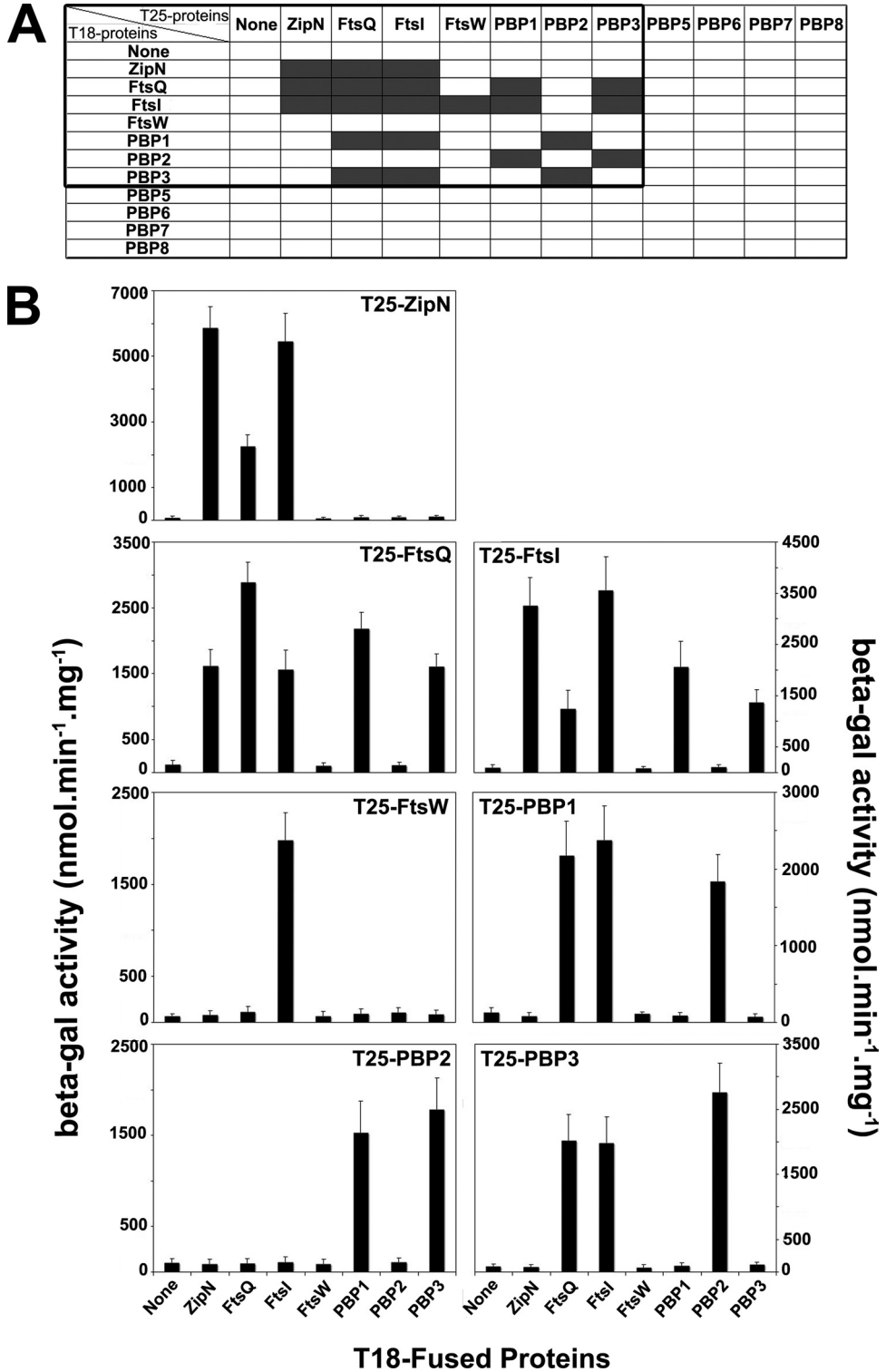

FIG. 6. Two-hybrid analysis of interactions between PBPs and the cytokinetic proteins FtsQ, FtsW, and ZipN. The occurrence of interaction between the tested proteins coproduced in *E. coli* DHM1 cells of the BACTH system was ascertained by the production of the β-galactosidase reporter enzyme whose activity (i) turned the corresponding cells (indicated by the gray rectangles in panel A) blue on X-Gal-containing medium and (ii) reached a high value (B; beta-gal). Each bar represents the mean value of two measurements performed on the cellular extracts of three reporter clones originating from independent transformations, and the error bars represent the standard deviation. Cells producing the two interacting ZipN-fusion proteins were used as the positive control (5,900 ± 750 β-Gal units), while those producing a single or no reporter protein served as the negative controls (65 ± 50 U of background β-Gal activity).

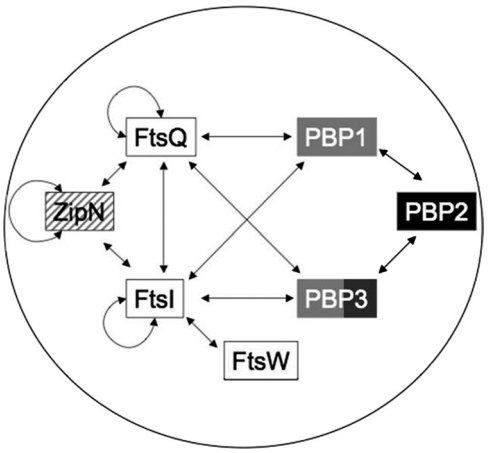

FIG. 7. Schematic representation of the web of interactions among the 10 presently studied proteins and ZipN, the cytokinetic factor we previously characterized. The spherical morphology of *Synechocystis* is represented by the circle. The double arrows indicate the presently reported interactions. Black and white letters stand for the proteins respectively indispensable and dispensable to *Synechocystis*. Black and white squares indicate that the corresponding mutants display decreased and increased cell sizes, respectively. Gray rectangles indicate that the corresponding mutants do not show any morphological defects. The hatched rectangle reminds us that the ZipN-depleted mutant has an aberrant spiral shape (26).

ACKNOWLEDGMENTS

We thank Daniel Ladant (Pasteur Institute, Paris, France) for the gift of the BACTH system.

This work was supported in part by French Scientific "ANR Biosys06: SULFIRHOM." M.M. and C.S. were recipients of fellowships from the CEA (France), and K.M. was the recipient of thesis fellowships from the Algerian Ministry for Education.

REFERENCES

1. **Addinall, S. G., and B. Holland.** 2002. The tubulin ancestor, FtsZ, draughtsman, designer and driving force for bacterial cytokinesis. J. Mol. Biol. **318:** 219–236.
2. **den Blaauwen, T., M. A. de Pedro, M. Nguyen-Disteche, and J. A. Ayala.** 2008. Morphogenesis of rod-shaped sacculi. FEMS Microbiol. Rev. **32:**321–344.
3. **Di Lallo, G., M. Fagioli, D. Barionovi, P. Ghelardini, and L. Paolozzi.** 2003. Use of a two-hybrid assay to study the assembly of a complex multicomponent protein machinery: bacterial septosome differentiation. Microbiology **149:**3353–3359.
4. **Domain, F., L. Houot, F. Chauvat, and C. Cassier-Chauvat.** 2004. Function and regulation of the cyanobacterial genes *lexA*, *recA* and *ruvB*: LexA is critical to the survival of cells facing inorganic carbon starvation. Mol. Microbiol. **53:**65–80.
5. **Ebersbach, G., E. Galli, J. Moller-Jensen, J. Lowe, and K. Gerdes.** 2008. Novel coiled-coil cell division factor ZapB stimulates Z ring assembly and cell division. Mol. Microbiol. **68:**720–735.
6. **Errington, J., R. A. Daniel, and D.-J. Scheffers.** 2003. Cytokinesis in bacteria. Microbiol. Mol. Biol. Rev. **67:**52–65.
7. **Ferris, M., and B. Palenik.** 1998. Niche adaptation in ocean cyanobacteria. Nature **396:**226–228.
8. **Gerdes, K., J. Moller-Jensen, G. Ebersbach, T. Kruse, and K. Nordstrom.** 2004. Bacterial mitotic machineries. Cell **116:**359–366.
9. **Glynn, J. M., J. E. Froehlich, and K. W. Osteryoung.** 2008. *Arabidopsis* ARC6 coordinates the division machineries of the inner and outer chloroplast membranes through interaction with PDV2 in the intermembrane space. Plant Cell **20:**2460–2470.
10. **Goehring, N. W., and J. Beckwith.** 2005. Diverse paths to midcell: assembly of the bacterial cell division machinery. Curr. Biol. **15:**R514–R526.
11. **Harry, E., L. Monahan, and L. Thompson.** 2006. Bacterial cell division: the mechanism and its precision. Int. Rev. Cytol. **253:**27–94.
12. **Haydon, D. J., N. R. Stokes, R. Ure, G. Galbraith, J. M. Bennett, D. R. Brown, P. J. Baker, V. V. Barynin, D. W. Rice, S. E. Sedelnikova, J. R. Heal, J. M. Sheridan, S. T. Aiwale, P. K. Chauhan, A. Srivastava, A. Taneja, I. Collins, J. Errington, and L. G. Czaplewski.** 2008. An inhibitor of FtsZ with potent and selective anti-staphylococcal activity. Science **321:**1673–1675.
13. **Heckman, K. L., and L. R. Pease.** 2007. Gene splicing and mutagenesis by PCR-driven overlap extension. Nat. Protoc. **2:**924–932.
14. **Justice, S. S., D. A. Hunstad, L. Cegelski, and S. J. Hultgren.** 2008. Morphological plasticity as a bacterial survival strategy. Nat. Rev. Microbiol. **6:**162–168.
15. **Karimova, G., N. Dautin, and D. Ladant.** 2005. Interaction network among *Escherichia coli* membrane proteins involved in cell division as revealed by bacterial two-hybrid analysis. J. Bacteriol. **187:**2233–2243.
16. **Karimova, G., J. Pidoux, A. Ullmann, and D. Ladant.** 1998. A bacterial two-hybrid system based on a reconstituted signal transduction pathway. Proc. Natl. Acad. Sci. USA **95:**5752–5756.
17. **Karimova, G., C. Robichon, and D. Ladant.** 2009. Characterization of YmgF, a 72-residue inner membrane protein that associates with the *Escherichia coli* cell division machinery. J. Bacteriol. **191:**333–346.
18. **Koksharova, O. A., and C. P. Wolk.** 2002. Genetic tools for cyanobacteria. Appl. Microbiol. Biotechnol. **58:**123–137.
19. **Koksharova, O. A., and C. P. Wolk.** 2002. A novel gene that bears a DnaJ motif influences cyanobacterial cell division. J. Bacteriol. **184:**5524–5528.
20. **Labarre, J., F. Chauvat, and P. Thuriaux.** 1989. Insertional mutagenesis by random cloning of antibiotic resistance genes into the genome of the cyanobacterium *Synechocystis* strain PCC 6803. J. Bacteriol. **171:**3449–3457.
21. **Leaver, M., P. Dominguez-Cuevas, J. M. Coxhead, R. A. Daniel, and J. Errington.** 2009. Life without a wall or division machine in *Bacillus subtilis*. Nature **457:**849–853.
22. **Leganes, F., A. Blanco-Rivero, F. Fernandez-Pinas, M. Redondo, E. Fernandez-Valiente, Q. Fan, S. Lechno-Yossef, and C. P. Wolk.** 2005. Wide variation in the cyanobacterial complement of presumptive penicillin-binding proteins. Arch. Microbiol. **184:**234–248.
23. **Lutkenhaus, J.** 2007. Assembly dynamics of the bacterial MinCDE system and spatial regulation of the Z ring. Annu. Rev. Biochem. **76:**539–562.
24. **Maggi, S., O. Massidda, G. Luzi, D. Fadda, L. Paolozzi, and P. Ghelardini.** 2008. Division protein interaction web: identification of a phylogenetically conserved common interactome between *Streptococcus pneumoniae* and *Escherichia coli*. Microbiology **154:**3042–3052.
25. **Maple, J., C. Aldridge, and S. G. Moller.** 2005. Plastid division is mediated by combinatorial assembly of plastid division proteins. Plant J. **43:**811–823.
26. **Mazouni, K., F. Domain, C. Cassier-Chauvat, and F. Chauvat.** 2004. Molecular analysis of the key cytokinetic components of cyanobacteria: FtsZ, ZipN and MinCDE. Mol. Microbiol. **52:**1145–1158.
27. **Meberg, B. M., A. L. Paulson, R. Priyadarshini, and K. D. Young.** 2004. Endopeptidase penicillin-binding proteins 4 and 7 play auxiliary roles in determining uniform morphology of *Escherichia coli*. J. Bacteriol. **186:**8326–8336.
28. **Miyagishima, S. Y., C. P. Wolk, and K. W. Osteryoung.** 2005. Identification of cyanobacterial cell division genes by comparative and mutational analyses. Mol. Microbiol. **56:**126–143.
29. **Morlot, C., A. Zapun, O. Dideberg, and T. Vernet.** 2003. Growth and division of *Streptococcus pneumoniae*: localization of the high molecular weight penicillin-binding proteins during the cell cycle. Mol. Microbiol. **50:**845–855.
30. **Partensky, F., W. R. Hess, and D. Vaulot.** 1999. *Prochlorococcus*, a marine photosynthetic prokaryote of global significance. Microbiol. Mol. Biol. Rev. **63:**106–127.
31. **Pedersen, L. B., E. R. Angert, and P. Setlow.** 1999. Septal localization of penicillin-binding protein 1 in *Bacillus subtilis*. J. Bacteriol. **181:**3201–3211.
32. **Prentki, P., and H. M. Krisch.** 1984. In vitro insertional mutagenesis with a selectable DNA fragment. Gene **29:**303–313.
33. **Rippka, R., J. Deruelles, J. Waterbury, M. Herdman, and R. Stanier.** 1979. Generic assignements, strains histories and properties of pure culture of cyanobacteria. J. Genet. Microbiol. **111:**1–61.
34. **Sakr, S., R. Jeanjean, C.-C. Zhang, and T. Arcondeguy.** 2006. Inhibition of cell division suppresses heterocyst development in *Anabaena* sp. strain PCC 7120. J. Bacteriol. **188:**1396–1404.
35. **Sauvage, E., F. Kerff, M. Terrak, J. A. Ayala, and P. Charlier.** 2008. The penicillin-binding proteins: structure and role in peptidoglycan biosynthesis. FEMS Microbiol. Rev. **32:**234–258.
36. **Scheffers, D.-J., and M. G. Pinho.** 2005. Bacterial cell wall synthesis: new insights from localization studies. Microbiol. Mol. Biol. Rev. **69:**585–607.
37. **Tzagoloff, H., and R. Novick.** 1977. Geometry of cell division in *Staphylococcus aureus*. J. Bacteriol. **129:**343–350.
38. **Vollmer, W., D. Blanot, and M. A. de Pedro.** 2008. Peptidoglycan structure and architecture. FEMS Microbiol. Rev. **32:**149–167.
39. **Westling-Häggström, B., T. Elmros, S. Normark, and B. Winblad.** 1977. Growth pattern and cell division in *Neisseria gonorrhoeae*. J. Bacteriol. **129:** 333–342.
40. **Zehr, J. P., J. B. Waterbury, P. J. Turner, J. P. Montoya, E. Omoregie, G. F. Steward, A. Hansen, and D. M. Karl.** 2001. Unicellular cyanobacteria fix N2 in the subtropical North Pacific Ocean. Nature **412:**635–638.